Research Paper

Journal of Vascular Research

J Vasc Res 2016;53:72–82
DOI: 10.1159/000448734

Received: May 13, 2016
Accepted after revision: July 26, 2016
Published online: September 20, 2016

Antiangiogenic Therapy Induces Hepatic Tumor Vascular Network Rearrangement to Receive Perfusion via the Portal Vein and Hepatic Artery

Wonseok Kang[a] Joon Seok Lim[b, c] Mi-Suk Park[b, c] Gou Young Koh[d, e] Honsoul Kim[b, c]

[a]Division of Gastroenterology, Department of Medicine, Samsung Medical Center, Sungkyunkwan University School of Medicine, [b]Department of Radiology and [c]Research Institute of Radiological Science, Severance Hospital, Yonsei University College of Medicine, Seoul, and [d]National Research Laboratory of Vascular Biology and Stem Cells and [e]Graduate School of Medical Science and Engineering, Korea Advanced Institute of Science and Technology (KAIST), Daejeon, Korea

Key Words
Hepatic malignancy · Hepatocellular carcinoma · Antiangiogenic agents · Drug resistance · Angiography

Abstract
Purpose: Hepatic malignancies can easily develop resistance to antiangiogenic therapy, but the underlying mechanism remains poorly understood. This study explores whether antiangiogenic therapy influences the tumor vascular network and/or the vessels feeding the hepatic tumor. ***Methods:*** Mice implanted with Lewis lung carcinoma (LLC) cells were subcutaneously injected 3 times (once every other day starting 1 week after LLC implantation) with either an antiangiogenic agent [vascular endothelial growth factor (VEGF)-Trap] or control agent (bovine serum albumin) at a dose of 25 mg/kg before performing angiography. Hepatic arteriography and portography were performed using a vascular cast method with vascular latex. ***Results:*** Arteriography of the control-treated LLC-implanted mice showed marked staining of the mass with a prominent feeding artery, suggesting that the tumor is supplied by arterial perfusion. No significant staining was observed on portography. By contrast, 33% (n = 3/9) of the LLC-implanted mice treated with the antiangiogenic agent VEGF-Trap showed intratumoral staining during portography, indicating that these tumors received perfusion via the portal vein. ***Conclusion:*** Antiangiogenic treatment can induce rearrangement of the hepatic tumor vascular network to establish communication with the portal vein. This implies that hepatic tumors can develop resistance to antiangiogenic therapy by maintaining perfusion through portal venous perfusion.

Introduction

Angiogenesis (the growth of new blood vessels) is essential for tumor growth and dissemination, and has long been recognized as an attractive target for anticancer therapy. Hepatocellular carcinoma (HCC) is a hypervascular tumor with high microvessel density; antiangiogenic therapy appears as a promising treatment option for patients with HCC [1]. One of the major angiogenesis mediators is vascular endothelial growth factor (VEGF). HCC patients have been reported to show increased VEGF levels in serum and cancerous tissue [2], and elevated VEGF levels have been associated with

KARGER

E-Mail karger@karger.com
www.karger.com/jvr

1018–1172/16/0532–0072$39.50/0

Dr. Honsoul Kim
Department of Radiology, Yonsei University College of Medicine
50-1 Yonsei-ro, Seodaemun-gu
Seoul 120-752 (Korea)
E-Mail pine0205@yuhs.ac

more invasive tumors and poor outcomes after treatment [3].

Various strategies to block VEGF pathways using antiangiogenic agents and thereby suppress tumor angiogenesis have been tested or are currently used for the treatment of HCC and/or liver metastasis, such as VEGF-neutralizing monoclonal antibody (bevacizumab), soluble VEGF receptor (VEGF-Trap) and VEGF receptor tyrosine kinase inhibitors (sorafenib and sunitinib) [4, 5]. However, some patients do not respond to antiangiogenic agents and patients who do respond experience only modest and transient effects; as a consequence, only sorafenib has proved to have survival benefits for the treatment of HCC [4, 6, 7].

Antiangiogenic therapy can also sometimes provoke tumors to become more aggressive or induce a metastatic acceleration, but the underlying mechanism is poorly understood [8, 9]. Several theories exist to explain how tumors develop resistance to antiangiogenic therapy. These include evasive resistance (adaptation to the presence of antiangiogenic therapy), intrinsic resistance (endogenous resistance to angiogenic inhibitors) [6], disruption of tumor vasculature that triggers local tumor cell invasion and distant metastasis [9] and a conditioning effect induced by antiangiogenic therapy that changes the microenvironment to become more permissive to tumor extravasation [8]. However, no previous studies have investigated the hemodynamic aspects of resistance to antiangiogenic therapy in hepatic tumors.

The liver receives dual-input perfusion from the hepatic artery and the portal vein, which confers a unique hemodynamic profile in hepatic tumors. Normal liver parenchyma receives perfusion through portal venules and hepatic arterioles, which are paired structures. By contrast, advanced HCC receives circulation from aberrant arterioles [10–12]. We hypothesized that normal liver vessels and aberrant hepatic tumor-feeding vessels might respond differently to antiangiogenic agents, and that different reactions of normal liver vasculature and aberrant tumor vessels to antiangiogenic treatment might result in rearrangements of the tumor vascular network. If so, these responses might influence the outcomes of antiangiogenic therapy.

In this study, we used a latex dye angiography method to examine the perfusion source of tumor vascular networks in an experimentally produced mouse hepatic tumor model after administrating antiangiogenic therapy or control treatment. The purpose of this study was to explore whether antiangiogenic therapy can influence the hepatic tumor feeding vessels and/or their vascular network.

Materials and Methods

Mice

The Animal Care Committee of Severance Hospital (permit No. 2014-0199) and the Korea Advanced Institute of Science and Technology (KAIST, permit No. KA2011-28) approved this study. Pathogen-free C57BL/6J mice were purchased from Jackson Laboratories and bred in our pathogen-free animal facility. All animals were fed with a standard normal diet (PMI Lab Diet) ad libitum with free access to water. Male mice, aged 8–10 weeks, were used for this study.

Cell Lines and Reagents

The mouse Lewis lung carcinoma (LLC, catalog No. CRL-1642™) cell line was obtained from the American Type Culture Collection. This cell line has a syngeneic background to C57BL/6J strain mice.

Male C57BL/6J mice, aged 8–10 weeks, were anesthetized by intramuscular injection of a mixture of anesthetics (80 mg/kg ketamine and 12 mg/kg xylazine). Skin and peritoneal incisions were made at the midline of the upper abdomen to expose the left lateral lobe of the liver. An in vitro-cultured cell-line suspension (2.5×10^5 cells in 20 μl of phosphate-buffered saline) was loaded into a 20-gauge insulin syringe, and subcapsular implantation was conducted in the left lateral lobe of the liver. The incision was repaired with a 4–0 black silk suture.

VEGF-Trap (soluble VEGF receptor fusion protein designed to interfere with signaling pathways of VEGF-A and placenta-induced growth factor) was a kind gift from Professor Gou Young Koh at KAIST. VEGF-Trap recombinant protein was produced from stable CHO cell lines transfected with *VEGF-Trap* genes, and secreted VEGF-Trap was purified from supernatant as described previously [13].

Thirty-eight LLC-implanted mouse liver tumor models were successfully produced. They were divided into 2 groups, which were treated with either VEGF-Trap (treatment group, n = 19) or bovine serum albumin (BSA; control group, n = 19). Either VEGF-Trap or control (BSA) was subcutaneously injected at a dose of 25 mg/kg every other day starting 1 week after LLC implantation. Each mouse was treated 3 times with VEGF-Trap or BSA (on days 7, 9, and 11 after LLC implantation). Arteriography or portography was performed on day 13 after implantation.

Selective Arteriography and Portography of Hepatic Vessels

The BSA-treated control group (n = 19) was divided into 2 groups. One group was subjected to arteriography with latex dye (n = 10; 3 of these procedures failed) and the other group was subjected to portography with either latex dye or 2% Evans blue solution (n = 9; 2 of these procedures failed). The VEGF-Trap-treated group was divided into 2 groups. One group was subjected to arteriography with latex dye (n = 8; 2 of these procedures failed) and the other group was subjected to portography with either latex dye or 2% Evans blue solution (n = 11; 2 of these procedures failed). Therefore, a total of 13/18 arteriography procedures and 16/20 portography procedures were successfully conducted.

Anesthesia was achieved by intramuscular injection of a mixture of anesthetics (80 mg/kg ketamine and 12 mg/kg xylazine). Systemic arteriography was performed as described previously [14, 15]. Briefly, the anterior side of the chest was opened, and an outflow opening was made at the right atrium of the beating heart.

The left ventricle of the heart was punctured with a blunted 18-gauge needle, and a vascular latex dye (Connecticut Valley Biological Supply Co., Southampton, Mass., USA) was slowly and gently injected with a 10-ml syringe. To achieve portography [15, 16], a midline incision was made and the colon and small bowel were shifted to the left to expose the target vessels. Then, a 22-gauge angiocatheter was inserted into the main portal venous trunk, which was used for dye infusion. Next, an outflow opening was made at the right atrium of the heart. Portography was performed with either latex dye or Evans blue solution. A 2% Evans blue solution was prepared by dissolving the appropriate amount of dye powder (Sigma-Aldrich, Saint Louis, Mo., USA) in phosphate-buffered saline. Evans blue solution is a water-soluble dye; unlike latex dye, it can freely flow through capillaries to enter the vascular compart-

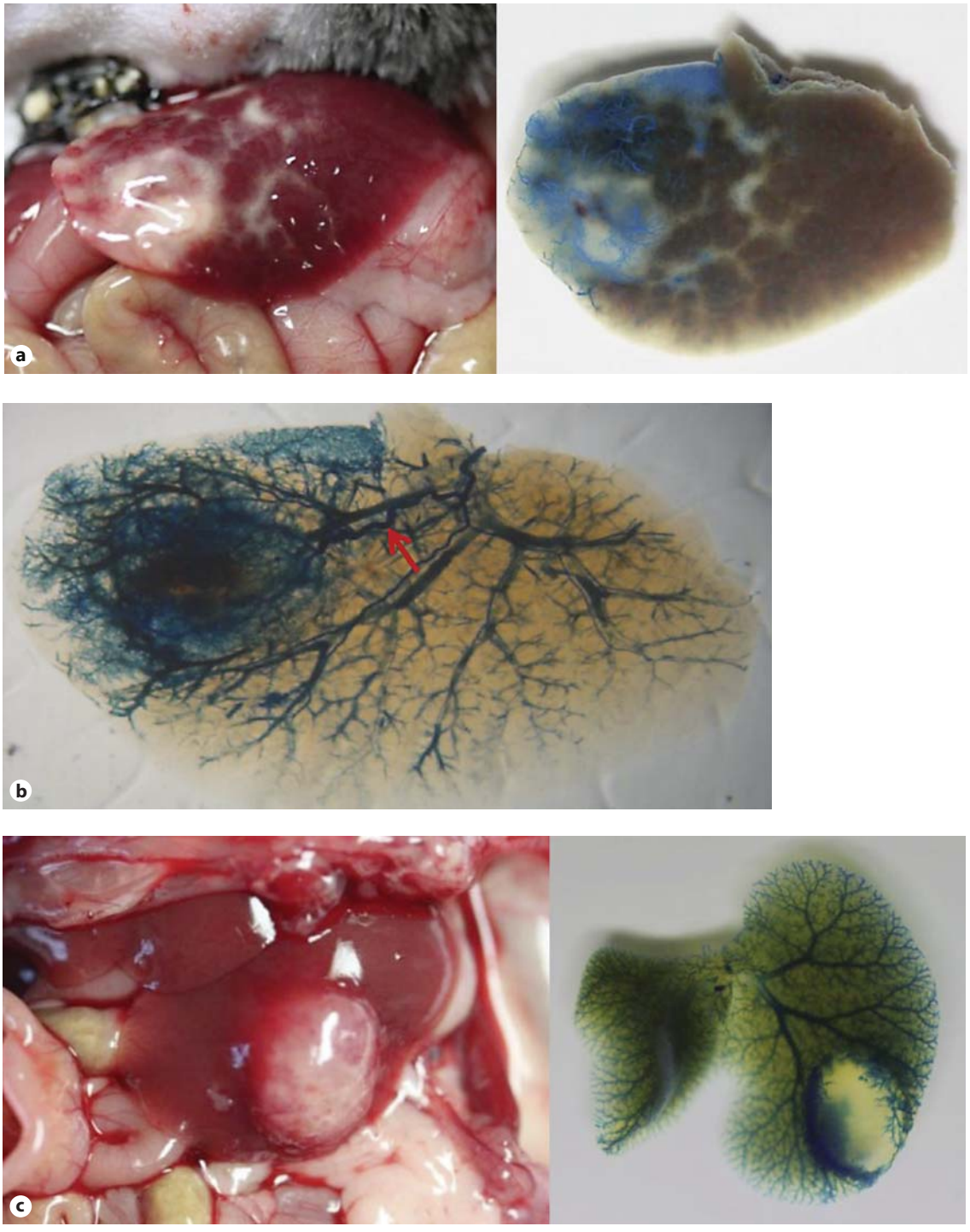

Color version available online

1

(For legend see next page.)

J Vasc Res 2016;53:72–82
DOI: 10.1159/000448734

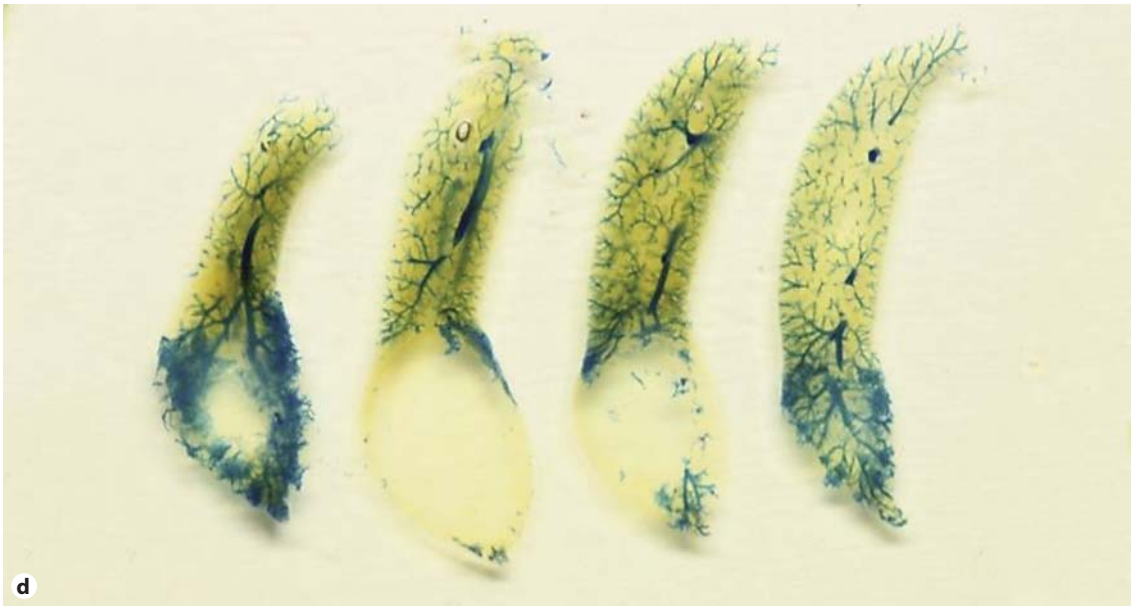

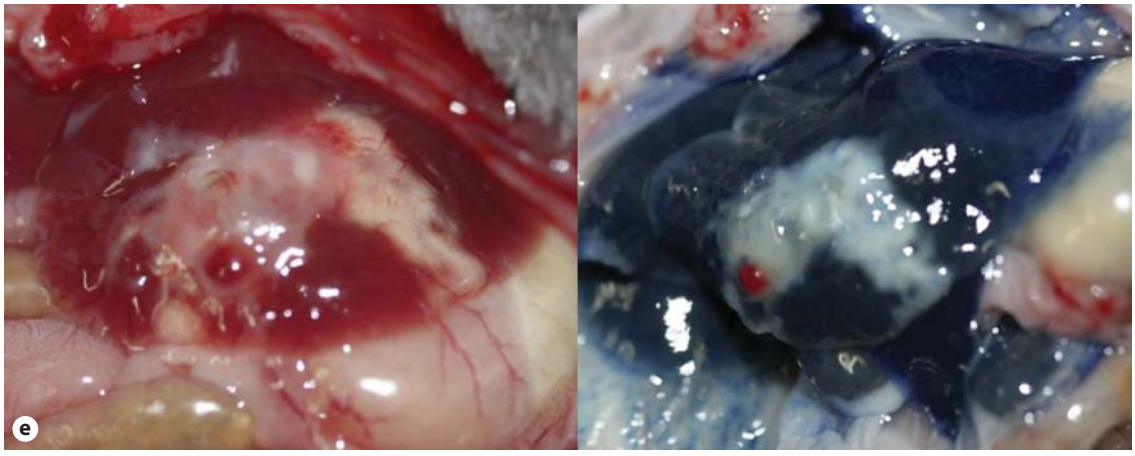

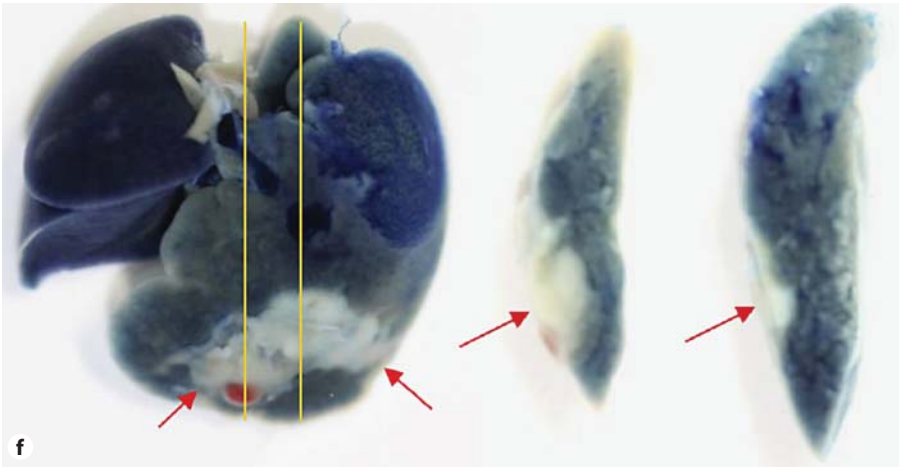

Fig. 1. Angiographic features of LLC-implanted mouse hepatic tumor model. **a** Images obtained before (left) and after (right) latex arteriography was performed. **b** The transparent specimen shows an enlarged tumor-feeding artery (arrow), which supplies a markedly hypervascular mass. **c** Gross images obtained before (left) and after (right) latex portography was performed. **d** The sectioned specimen shows that latex dye staining is limited to the junction of tumor and adjacent liver whereas the center of the mass is unstained. **e** Images obtained before (left) and after (right) portography with 2% Evans blue solution. **f** Evans blue staining is absent within the tumor (left), indicating that this tumor (arrow) is isolated from the portal vein; yellow lines represent the orientation of the sectioned specimen (right).

ments lying beyond the capillary bed. Therefore, before infusing Evans blue solution, the entire heart was clamped with a hemostat at a level just above the right atrium outflow opening to prevent contamination of nontargeted vascular compartments by re-entry of the Evans blue into the systemic circulation. Portography was performed by slowly and gently infusing either vascular latex dye or 2% Evans blue solution via the angiocatheter inserted into the main portal venous trunk.

The liver was resected and briefly washed in phosphate-buffered saline. The specimen was fixed with 10% formalin overnight. For whole-mount imaging of latex-perfused vessels, a tissue clearance procedure was performed to enhance sample transparency and maximize delineation of the vascular casts. The specimen was dehydrated by processing with a graded methanol series, and cleared by immersion into a mixture of organic solvent (benzyl alcohol:benzyl benzoate, 1:1, Sigma-Aldrich) [16].

Measurement of the Number of Intratumoral Vessels Containing Latex Dye

The tumor specimen was sliced at a thickness of approximately 5 mm and embedded in paraffin and then 5-μm-thick sections were cut using a microtome. Hematoxylin and eosin staining was performed. Multiple random microscopic fields at the central portion of the tumor were examined under magnification (×200), and the number of latex dye containing vessels was counted.

Statistical Analysis

Statistical analyses relied on standard software (SPSS v19; SPSS Inc., Chicago, Ill., USA). Student's t test was used for evaluating the difference of the number of intratumoral vessels containing latex dye. Statistical significance was set at $p < 0.05$.

Results

Angiographic Features of LLC-Implanted Mouse Hepatic Tumors and Human HCC Are Similar

Latex arteriography of the BSA-treated LLC-implanted hepatic tumor model presented the tumor as a markedly hypervascular mass. The tumor mass was supplied by a prominent tumor-feeding vessel, which arose from the hepatic artery (n = 7; fig. 1a, b). Microscopic examination revealed multiple dilated vessels containing blue latex particles (online suppl. fig. 1A; for all online suppl. material, see www.karger.com/doi/10.1159/000448734).

Latex portography of BSA-treated LLC-implanted mice showed that latex dye did not enter the mass, but prominent staining occurred at the junction of the mass and liver (n = 4; fig. 1c, d). Upon microscopic examination, multiple dilated vessels containing blue latex particles were observed within the liver and at the peripheral portion of the mass near the liver-tumor junction (online suppl. fig. 1B), but rarely at the central portion of the tumor (online suppl. fig. 1C). We counted the number of blue latex dye-containing vessels within random microscopic fields (magnification ×200) at the central portion of the tumor and found 0.24 ± 0.49 vessels (mean ± standard deviation) per field. The latex dye cannot pass through to the capillary vessels [14]; therefore, we could not determine whether the mass capillaries were isolated from the portal vein or whether the capillaries between portal venules and the tumor were too small for the latex dye to enter. We repeated portal perfusion using 2% Evans blue solution instead of latex dye (n = 3), and confirmed the absence of dye staining within the mass (fig. 1e, f).

Antiangiogenic Therapy Induces Rearrangement of the Tumor Vascular Network

Latex arteriography and latex portography were repeated in LLC-implanted mice treated with VEGF-Trap. Latex arteriography (n = 6) did not detect significant arterial alterations in most cases (n = 5; online suppl. fig. 2) compared with control mice, but 1 VEGF-Trap-treated mouse displayed sparse intratumoral vessels (16.7%, n = 1/6; online suppl. fig. 3). Next, we performed latex portography (n = 6) in the VEGF-Trap-treated LLC-implanted mice. Unlike the control mice, which did not receive significant portal venous perfusion, some (n = 2) of the VEGF-Trap-treated LLC-implanted mice had diffuse dye within the intratumoral vessels (fig. 2a–c). Microscopic assessment also confirmed the presence of blue latex dye particles within vessels of the tumor central portion (fig. 2d). The number of vessels containing blue latex particles per random microscopic field (magnification ×200; mean ± standard deviation 3.52 ± 1.34) in these mice was significantly higher ($p < 0.001$, fig. 2e) than that of the BSA-treated control mice (mean ± standard deviation 0.24 ± 0.49). We repeated portography using 2% Evans blue solution (n = 3) instead of latex dye (fig. 2f, g), and again observed perfusion of the mass in 1 mouse. Collectively, we observed dye staining during photography using either latex or 2% Evans blue solution in 33% (n = 3/9) of the LLC-implanted mice treated with VEGF-Trap.

Discussion

Antiangiogenic therapies are designed to suppress tumor angiogenesis and destroy pre-existing tumor vessels, and are widely used for the treatment of various malignancies. However, the tumor microenvironment can change in response to antiangiogenic therapy, which results in resistance to antiangiogenic drugs and agents [17]. Tumor vasculatures frequently present as abnormal

and chaotic leaky structures with stagnant perfusion. VEGF inhibition induces vascular remodeling by reducing vessel size and tortuosity, and the remaining tumor vessels show improved pericyte coverage and normalized basement membranes [13, 18–20]. The clinical significance of such phenomena is poorly understood. Although there is ongoing debate, some studies suggest that vascular normalization and maturation may represent a process of therapeutic escape and tumor progression [21].

In addition to inducing vascular structural alterations, antiangiogenic therapies are associated with hemodynamic changes. Previous studies on the effects of antian-

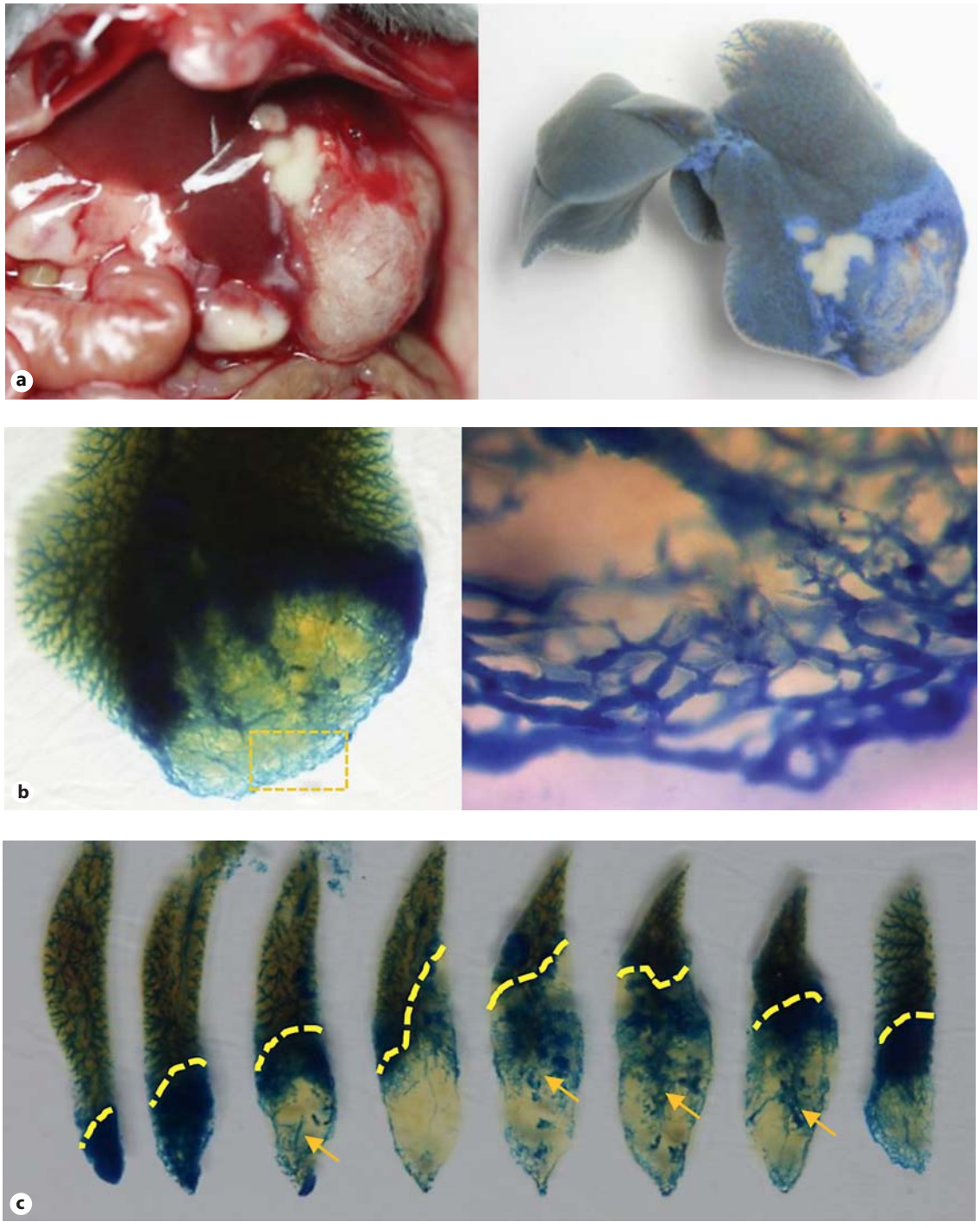

Color version available online

2

(For legend see next page.)

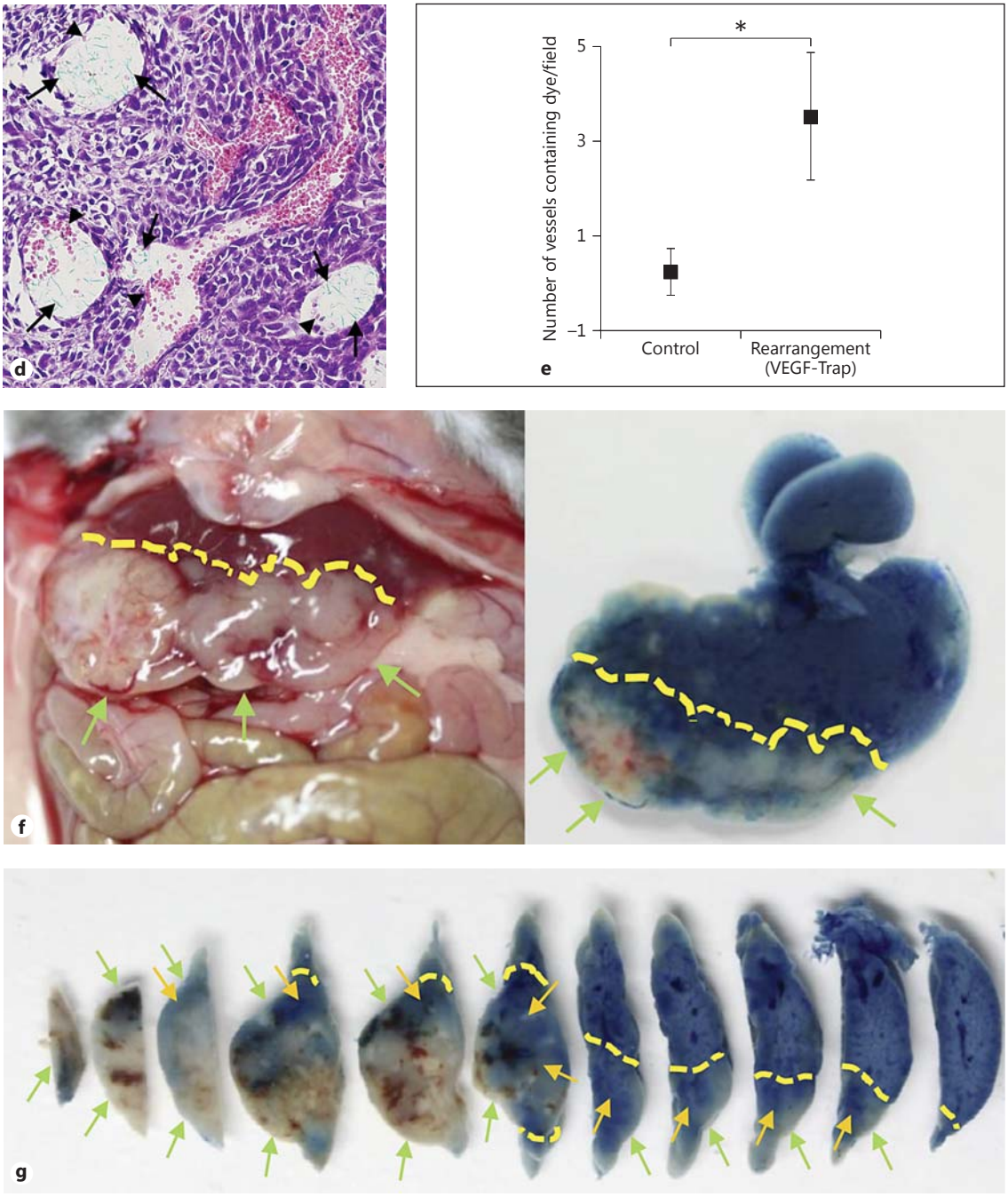

Fig. 2. Portography of LLC-implanted mice after VEGF-Trap treatment. Portography was performed using latex dye (**a–d**) or 2% Evans blue solution (**e**, **f**). **a** Images obtained before (left) and after (right) performing latex portography. **b** Gross specimen image (left) and magnified specimen image (right) after performing tissue clearance. The magnified area is indicated with dotted lines in the inset. **c** Sectioned specimen images. Dotted line demarcates the margin of tumor. Orange arrow indicates intratumoral blue latex dye staining. **d** Histological examination reveals latex dye particles (blue, indicated with arrows) within an intratumoral vessel. Arrowheads indicate red blood cells. HE. ×200. **e** Comparison of the number of vessels containing blue latex particles counted per microscopic field (×200) at the central portion of tumor after latex portography obtained from the BSA-treated control mice and the mice which showed intratumoral staining after VEGF-Trap treatment (* $p < 0.001$). **f** Images obtained before (left) and after (right) performing portography using 2% Evans blue solution. Latex dye (orange arrow) is seen within the central portion of the tumor. **g** Sectioned specimen images. Dotted line demarcates the margin (indicated with arrows) of tumor (green arrow). Orange arrow indicates intratumoral Evans blue staining.

giogenic agents on human HCC using perfusion computed tomography (CT), magnetic resonance imaging (MRI) and contrast-enhanced ultrasonography describe several significant hemodynamic features of tumors. For example, patients showing good treatment responses have less perfusion heterogeneity [22] a higher baseline mean transit time and transfer constant (K_{trans}) [23] and an early reduction in tumor vascularity and blood volume [24].

This study aimed to elucidate the mechanism underlying the resistance of hepatic tumors (primarily HCC, but also applicable to other malignancies such as hypervascular metastasis) to antiangiogenic agents, focusing particularly on the tumor-feeding vessel and associated perfusion alterations. In our previous study, we examined several mouse hepatic tumor models, and concluded that the LLC-implanted ectopic tumor model closely simulates the angiographic features of human HCC [15]. The LLC-implanted mouse hepatic tumor model was hypervascular, and angiography revealed that the tumor received arterial perfusion but avoided portal venous perfusion. Similar angiographic features have also been described in a radiation-induced fibrosarcoma cell line liver implantation model, which demonstrated a portal flow void to the tumor during digital microangiography performed after barium suspension infusion [25]. These are typical angiographic features of human HCC [26–28], but the increase in arterial perfusion, along with the decrease in portal perfusion, is an event that can also take place in liver metastasis [28, 29]. Consequently, we believe that our liver LLC-implanted tumor model can simulate both human HCC and hypervascular liver metastasis.

To differentiate the origin of tumor-feeding vessels and intratumoral vessels that arise from the hepatic artery and/or portal vein, we applied a commercial latex dye used for vascular experiments and produced vascular casts [14, 15]. This approach enabled us to perform compartment-specific latex arteriography and portography, and visualize the tumor-feeding vessels and/or their supplied tissues in a manner similar to that used for human conventional angiography. After administration of VEGF-Trap and subsequent portography, a modest percentage of the mice (33%, n = 3/9) showed intratumoral vessel staining, which we interpreted as the development of communication between tumor vessels and intrahepatic portal venules. We believe that this is due to rearrangement of the tumor vascular network from an arterial system to a dual vessel system, which establishes communication with the hepatic artery and the portal vein (fig. 3). This scenario may provide a hemodynamic mechanism, explaining why some liver tumors that do not respond to antiangiogenic therapy maintain their perfusion and gain resistance.

Implantation of VX2 carcinoma into the rabbit liver produces a hepatic tumor model with a similar blood supply pattern to that of human HCC [30, 31]. Stewart et al. [32] used this model and reported that CT perfusion studies performed 8 days after thalidomide (angiogenesis inhibitor) administration yield results that can be used to predict treatment response. In their study, animals treated with thalidomide were divided into 2 groups: responders had a reduction in tumor perfusion whereas nonresponders had no significant change in tumor perfusion. Responders also had an improvement in progression-free survival and reduced microvessel density compared to nonresponders [32]. Liver-implanted VX2 tumors contain a mixture of portal vein and hepatic arterioles [30]. Based on the portal vein communication with tumor vessels, we assume that tumor vascular rearrangement might also have occurred in the VX2-implanted model based on the portal vein communication with the tumor vessels, and might have contributed, at least in part, to maintaining tumor perfusion in nonresponders.

In human HCC, capillaries of the tumor periphery frequently maintain communication with the adjacent liver sinusoid vessels [26]. Therefore, we believe that if tumor arterial perfusion is suppressed by antiangiogenic therapy, then perfusion rearrangement may occur to receive portal venous blood via liver sinusoidal vessels. A few clinical reports described similar perfusion alterations in HCC patients treated with transarterial chemoembolization (TACE), in which the tumor-feeding vessels that were initially supplied by the hepatic artery became rearranged to partially receive portal venous perfusion after embolization of the tumor-feeding arteries [33, 34].

Our concept of tumor vascular network (perfusion) rearrangement induced by antiangiogenic therapy has an important clinical implication. TACE is currently a primary therapeutic option, especially for unresectable HCC patients [35]. If the HCC tumor receives perfusion from the portal vein, then the efficacy of TACE becomes significantly jeopardized. Unlike the hepatic artery, the portal vein cannot be approached via a superficial vascular route. If the tumor receives blood from the portal vein in addition to the hepatic artery, then TACE treatment becomes incomplete because it only embolizes the tumor-feeding artery.

In our study, 1 mouse (16.7%) had a marked reduction in tumor vascular staining on latex arteriography, which might represent pruning of tumor arterioles. This was an unexpected result because we considered vascular prun-

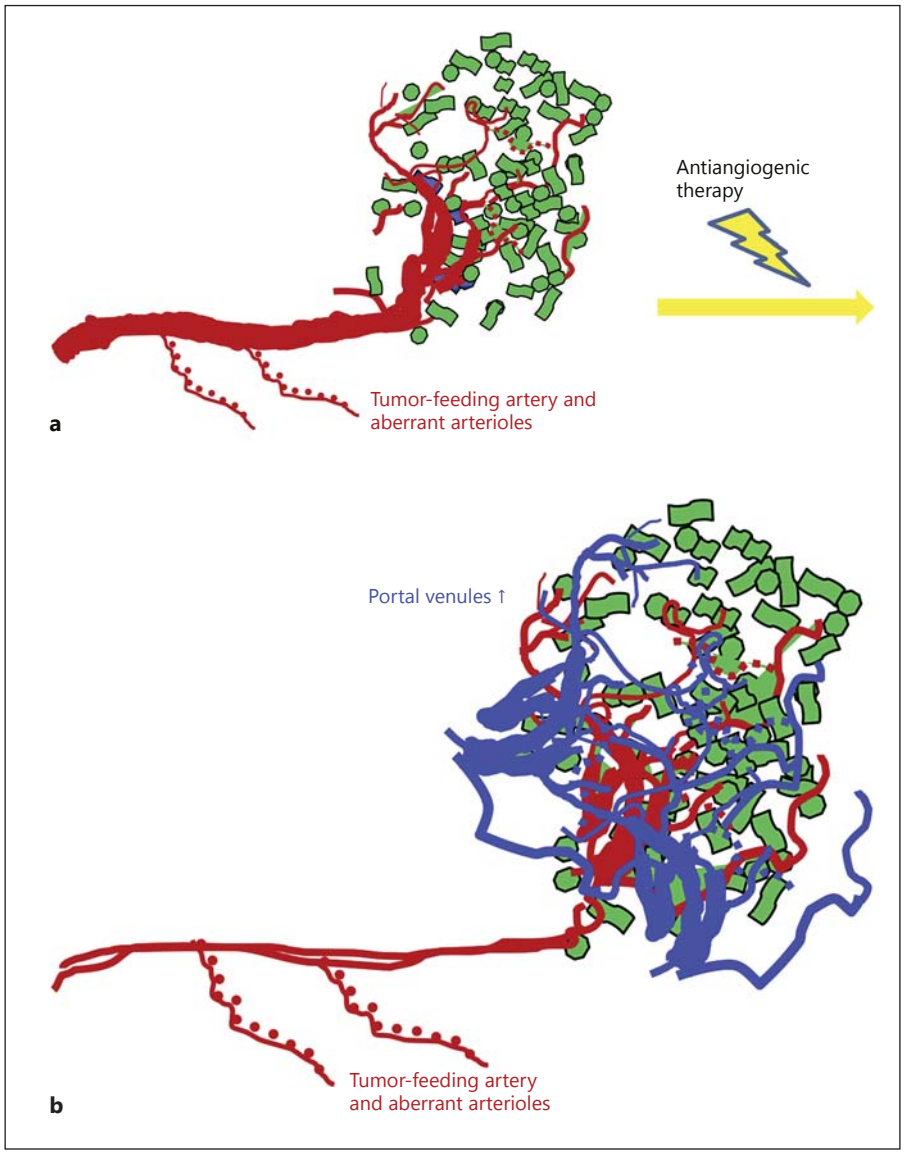

Fig. 3. A schematic diagram illustrates a model for tumor vascular network rearrangement induced by antiangiogenic therapy. **a** A fully developed hepatocellular carcinoma typically is supplied by tumor-feeding arteries and aberrant arterioles, but is devoid of portal venous perfusion. **b** Antiangiogenic treatment can induce tumor vascular network rearrangement so that it receives portal venous perfusion in addition to arterial perfusion from the tumor-feeding artery.

ing and normalization as events on the level of the capillaries, which are vessels that are too small for the latex dye to enter. Therefore, we considered that latex arteriography would not demonstrate a significant phenotype regardless of whether or not changes in microvessel structure do occur. Currently, we are hesitant to validate this event, which was observed in only 1 mouse. This observation does not affect the main conclusion of the study regarding the observed rearrangement of the tumor vascular network which led to establishing communication with the portal vein.

We believe that our results support previous theories on tumor hypoxia, evasive resistance to antiangiogenic therapies and/or more aggressive tumor growth after antiangiogenic therapies. Many researchers report that tissue hypoxia in response to antiangiogenic therapy enhances tumor aggressiveness. Hypoxia-inducible factor 1α (HIF-1α) and HIF-2α are responsible for resistance to antiangiogenic therapy [36, 37]. If hypoxia is an important factor, we believe that tumor vascular network rearrangement to receive relatively deoxygenated portal venous blood would be an efficient way to subject the tumor to hypoxic conditions. Portal venous blood also contains rich nutrition absorbed from the small intestines, which the tumor can use to fuel aggressive growth.

We recognize 3 limitations in our study. First, we selected the LLC-implanted tumor model based on its similarities to HCC with respect to tumor-feeding vessels and angiographic characteristics. We acknowledge that the nature of this model can differ from that of human HCC. However, we justify our choice by the fact that it was based on the results of our previous study which examined several liver tumor models [15], and that it serves as a liver hypervascular metastasis model. Second, we were not able to provide mechanistic and histological evaluations to support our conclusion. The process of latex perfusion and tissue clearance with organic solvents converted the tissue's physical consistency, and specimens with vascular rearrangement could not be used for further biochemical and/or physiological analyses. Third, the latex angiography method we used is an ex vivo method that cannot be used for serial imaging. Therefore, we were not able to compare the vascular state before and after performing antiangiogenic therapy.

In conclusion, we adopted a liver tumor model, in which the angiographic features of the tumor-feeding vessels resemble those of human HCC and hypervascular metastasis, in order to study the effects of antiangiogenic treatment on tumor vasculature. The results indicate that antiangiogenic treatment can cause the solely arterialized tumor vascular network to rearrange and simultaneously receive portal venous blood and arterial blood. This phenomenon provides a hemodynamic explanation for how hepatic tumors (including but not limited to HCC) maintain perfusion, despite antiangiogenic treatment, and ultimately gain resistance to antiangiogenic therapies.

Disclosure Statement

The authors have no potential conflicts of interest to declare. The authors received no specific funding for this work.

References

1 Zhu AX, Raymond E: Early development of sunitinib in hepatocellular carcinoma. Expert review of anticancer therapy 2009;9:143–150.
2 Moon WS, Rhyu KH, Kang MJ, Lee DG, Yu HC, Yeum JH, Koh GY, Tarnawski AS: Overexpression of VEGF and angiopoietin 2: a key to high vascularity of hepatocellular carcinoma? Mod Pathol 2003;16:552–557.
3 Poon RT, Lau C, Pang R, Ng KK, Yuen J, Fan ST: High serum vascular endothelial growth factor levels predict poor prognosis after radiofrequency ablation of hepatocellular carcinoma: importance of tumor biomarker in ablative therapies. Ann Surg Oncol 2007;14:1835–1845.
4 Wenger JB, Santos N, Liu Y, Dallas J, Subbiah S, Hochwald S, Huang EH, Dang DT, Allegra CJ, Luesch H, Dang LH: Can we develop effective combination antiangiogenic therapy for patients with hepatocellular carcinoma? Oncol Rev 2011;5:177–184.
5 Finn RS: Emerging targeted strategies in advanced hepatocellular carcinoma. Semin Liver Dis 2013;33(Suppl 1):S11–S19.
6 Bergers G, Hanahan D: Modes of resistance to anti-angiogenic therapy. Nat Rev Cancer 2008;8:592–603.
7 Llovet JM, Ricci S, Mazzaferro V, Hilgard P, Gane E, Blanc JF, de Oliveira AC, Santoro A, Raoul JL, Forner A, Schwartz M, Porta C, Zeuzem S, Bolondi L, Greten TF, Galle PR, Seitz JF, Borbath I, Haussinger D, Giannaris T, Shan M, Moscovici M, Voliotis D, Bruix J; SHARP Investigators Study Group: Sorafenib in advanced hepatocellular carcinoma. N Engl J Med 2008;359:378–390.
8 Ebos JM, Lee CR, Cruz-Munoz W, Bjarnason GA, Christensen JG, Kerbel RS: Accelerated metastasis after short-term treatment with a potent inhibitor of tumor angiogenesis. Cancer Cell 2009;15:232–239.
9 Paez-Ribes M, Allen E, Hudock J, Takeda T, Okuyama H, Vinals F, Inoue M, Bergers G, Hanahan D, Casanovas O: Antiangiogenic therapy elicits malignant progression of tumors to increased local invasion and distant metastasis. Cancer Cell 2009;15:220–231.
10 Himeno H, Enzan H, Saibara T, Onishi S, Yamamoto Y: Hitherto unrecognized arterioles within hepatocellular carcinoma. J Pathol 1994;174:217–222.
11 Matsui O, Kobayashi S, Sanada J, Kouda W, Ryu Y, Kozaka K, Kitao A, Nakamura K, Gabata T: Hepatocelluar nodules in liver cirrhosis: hemodynamic evaluation (angiography-assisted CT) with special reference to multistep hepatocarcinogenesis. Abdom Imaging 2011;36:264–272.
12 Park YN, Kim YB, Yang KM, Park C: Increased expression of vascular endothelial growth factor and angiogenesis in the early stage of multistep hepatocarcinogenesis. Arch Pathol Lab Med 2000;124:1061–1065.
13 Koh YJ, Kim HZ, Hwang SI, Lee JE, Oh N, Jung K, Kim M, Kim KE, Kim H, Lim NK, Jeon CJ, Lee GM, Jeon BH, Nam DH, Sung HK, Nagy A, Yoo OJ, Koh GY: Double antiangiogenic protein, DAAP, targeting VEGF-A and angiopoietins in tumor angiogenesis, metastasis, and vascular leakage. Cancer Cell 2010;18:171–184.
14 Park SO, Wankhede M, Lee YJ, Choi EJ, Fliess N, Choe SW, Oh SH, Walter G, Raizada MK, Sorg BS, Oh SP: Real-time imaging of de novo arteriovenous malformation in a mouse model of hereditary hemorrhagic telangiectasia. J Clin Invest 2009;119:3487–3496.
15 Kim SK, Kim H, Koh GY, Lim DS, Yu DY, Kim MD, Park MS, Lim JS: Mouse hepatic tumor vascular imaging by experimental selective angiography. PLoS One 2015;10:e0131687.
16 Walter TJ, Sparks EE, Huppert SS: 3-dimensional resin casting and imaging of mouse portal vein or intrahepatic bile duct system. J Vis Exp 2012;68:e4272.
17 Bottsford-Miller JN, Coleman RL, Sood AK: Resistance and escape from antiangiogenesis therapy: clinical implications and future strategies. J Clin Oncol 2012;30:4026–4034.
18 Tong RT, Boucher Y, Kozin SV, Winkler F, Hicklin DJ, Jain RK: Vascular normalization by vascular endothelial growth factor receptor 2 blockade induces a pressure gradient across the vasculature and improves drug penetration in tumors. Cancer Res 2004;64:3731–3736.
19 Carmeliet P, Jain RK: Principles and mechanisms of vessel normalization for cancer and other angiogenic diseases. Nat Rev Drug Discov 2011;10:417–427.
20 De Bock K, Cauwenberghs S, Carmeliet P: Vessel abnormalization: another hallmark of cancer? Molecular mechanisms and therapeutic implications. Curr Opin Genet Dev 2011;21:73–79.

21 Stockmann C, Doedens A, Weidemann A, Zhang N, Takeda N, Greenberg JI, Cheresh DA, Johnson RS: Deletion of vascular endothelial growth factor in myeloid cells accelerates tumorigenesis. Nature 2008;456:814–818.
22 Hayano K, Lee SH, Yoshida H, Zhu AX, Sahani DV: Fractal analysis of CT perfusion images for evaluation of antiangiogenic treatment and survival in hepatocellular carcinoma. Acad Radiol 2014;21:654–660.
23 Jiang T, Kambadakone A, Kulkarni NM, Zhu AX, Sahani DV: Monitoring response to antiangiogenic treatment and predicting outcomes in advanced hepatocellular carcinoma using image biomarkers, CT perfusion, tumor density, and tumor size (RECIST). Invest Radiol 2012;47:11–17.
24 Lassau N, Koscielny S, Chami L, Chebil M, Benatsou B, Roche A, Ducreux M, Malka D, Boige V: Advanced hepatocellular carcinoma: early evaluation of response to bevacizumab therapy at dynamic contrast-enhanced US with quantification – preliminary results. Radiology 2011;258:291–300.
25 Wang H, Van de Putte M, Chen F, De Keyzer F, Jin L, Yu J, Marchal G, de Witte P, Ni Y: Murine liver implantation of radiation-induced fibrosarcoma: characterization with MR imaging, microangiography and histopathology. Eur Radiol 2008;18:1422–1430.
26 Kitao A, Zen Y, Matsui O, Gabata T, Nakanuma Y: Hepatocarcinogenesis: multistep changes of drainage vessels at CT during arterial portography and hepatic arteriography – radiologic-pathologic correlation. Radiology 2009;252:605–614.
27 Hayashi M, Matsui O, Ueda K, Kawamori Y, Gabata T, Kadoya M: Progression to hypervascular hepatocellular carcinoma: correlation with intranodular blood supply evaluated with CT during intra-arterial injection of contrast material. Radiology 2002;225:143–149.
28 Thng CH, Koh TS, Collins DJ, Koh DM: Perfusion magnetic resonance imaging of the liver. World J Gastroenterol 2010;16:1598–1609.
29 Leggett DA, Kelley BB, Bunce IH, Miles KA: Colorectal cancer: diagnostic potential of CT measurements of hepatic perfusion and implications for contrast enhancement protocols. Radiology 1997;205:716–720.
30 Pauser S, Wagner S, Lippmann M, Pohlen U, Reszka R, Wolf KJ, Berger G: Evaluation of efficient chemoembolization mixtures by magnetic resonance imaging therapy monitoring: an experimental study on the VX2 tumor in the rabbit liver. Cancer Res 1996;56:1863–1867.
31 Ma GL, Bai RJ, Jiang HJ, Hao XJ, Dong XP, Li DQ, Liu XD, Wei L: Early changes of hepatic hemodynamics measured by functional CT perfusion in a rabbit model of liver tumor. Hepatobiliary Pancreat Dis Int 2012;11:407–411.
32 Stewart EE, Sun H, Chen X, Schafer PH, Chen Y, Garcia BM, Lee TY: Effect of an angiogenesis inhibitor on hepatic tumor perfusion and the implications for adjuvant cytotoxic therapy. Radiology 2012;264:68–77.
33 Choi SH, Chung JW, Lee HS: Hepatocellular carcinoma supplied by portal flow after repeated transcatheter arterial chemoembolization. Am J Roentgenol 2003;181:889–890.
34 Goseki N, Nosaka T, Endo M, Koike M: Nourishment of hepatocellular carcinoma cells through the portal blood flow with and without transcatheter arterial embolization. Cancer 1995;76:736–742.
35 El-Serag HB: Hepatocellular carcinoma. N Engl J Med 2011;365:1118–1127.
36 Yao JC, Phan A, Hoff PM, Chen HX, Charnsangavej C, Yeung SC, Hess K, Ng C, Abbruzzese JL, Ajani JA: Targeting vascular endothelial growth factor in advanced carcinoid tumor: a random assignment phase II study of depot octreotide with bevacizumab and pegylated interferon alpha-2b. J Clin Oncol 2008;26:1316–1323.
37 Ellis LM, Hicklin DJ: VEGF-targeted therapy: mechanisms of anti-tumour activity. Nat Rev Cancer 2008;8:579–591.